Science of the Total Environment 929 (2024) 172757

Contents lists available at ScienceDirect

Science of the Total Environment

journal homepage: www.elsevier.com/locate/scitotenv

# Ecotoxicological evaluation of chitosan biopolymer films particles in adult zebrafish (*Danio rerio*): A comparative study with polystyrene microplastics

Selene Elizabeth Herrera-Vázquez [a,1], Gustavo Axel Elizalde-Velázquez [a,1], Leobardo Manuel Gómez-Oliván [a,*], José Jorge Chanona-Pérez [b], Josué David Hernández-Varela [b], Misael Hernández-Díaz [c], Sandra García-Medina [c], José Manuel Orozco-Hernández [a], Karla Colín-García [a]

[a] *Laboratorio de Toxicología Ambiental, Facultad de Química, Universidad Autónoma del Estado de México, Paseo Colón intersección Paseo Tollocan, Colonia Residencial Colón, CP 50120 Toluca, Estado de México, Mexico*

[b] *Departamento de Ingeniería Bioquímica, Escuela Nacional de Ciencias Biológicas, Instituto Politécnico Nacional, Unidad Profesional Adolfo López Mateos, Av. Wilfrido Massieu s/n y cerrada Manuel Stampa, Col. Industrial Vallejo, Ciudad de México CP 07700, Mexico*

[c] *Laboratorio de Toxicología Acuática, Departamento de Farmacia, Escuela Nacional de Ciencias Biológicas, Instituto Politécnico Nacional, Unidad Profesional Adolfo López Mateos, Av. Wilfrido Massieu s/n y cerrada Manuel Stampa, Col. Industrial Vallejo, Ciudad de México CP, 07700, Mexico*

## HIGHLIGHTS

- Biopolymeric films do not prompt a severe toxic response in zebrafish organs.
- All evaluated organs undergone deleterious effects after microplastic exposure.
- Polystyrene microspheres were observed in gills and gut of zebrafish.
- Tissue damage was attributed to the presence of microspheres in the gut and gills.

## GRAPHICAL ABSTRACT

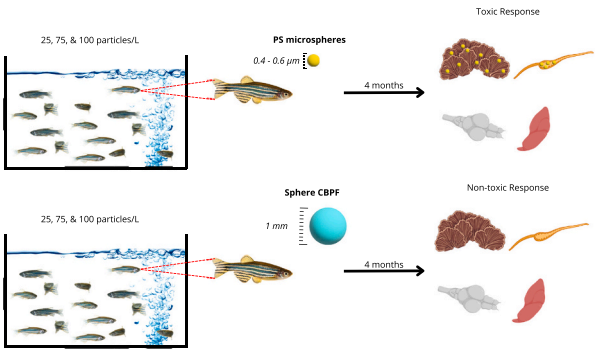


## ARTICLE INFO

Editor: Daniela Maria Pampanin

*Keywords:*
Microplastics
Biodegradable polymers
Toxic effects
Oxidative damage
Gene expression

## ABSTRACT

To mitigate the environmental impact of microplastics (MPs), the scientific community has innovated sustainable and biodegradable polymers as viable alternatives to traditional plastics. Chitosan, the deacetylated form of chitin, stands as one of the most thoroughly investigated biopolymers and has garnered significant interest due to its versatile applications in both medical and cosmetic fields. Nevertheless, there is still a knowledge gap regarding the impact that chitosan biopolymer films (CBPF) may generate in aquatic organisms. In light of the foregoing, this study aimed to assess and compare the potential effects of CBPF on the gastrointestinal tract, gills, brain, and liver of *Danio rerio* against those induced by MPs. The findings revealed that both CBPF and MPs induced changes in the levels of oxidative stress biomarkers across all organs. However, it is essential to note that

* Corresponding author.
*E-mail address:* lmgomezo@uaemex.mx (L.M. Gómez-Oliván).
[1] These authors contributed equally

https://doi.org/10.1016/j.scitotenv.2024.172757
Received 29 February 2024; Received in revised form 16 April 2024; Accepted 23 April 2024
Available online 24 April 2024

our star plots illustrate a tendency for CBPF to activate antioxidant enzymes and for MPs to produce oxidative damage. Regarding gene expression, our findings indicate that MPs led to an up-regulation in the expression of genes associated with apoptotic response (p53, casp3, cas9, bax, and bcl2) in all fish organs. Meanwhile, CBPF produced the same effect in genes related to antioxidant response (nrf1 and nrf2). Overall, our histological observations substantiated these effects, revealing the presence of plastic particles and tissue alterations in the gills and gastrointestinal tract of fish subjected to MPs. From these results, it can be concluded that CBPF does not represent a risk to fish after long exposure.

## 1. Introduction

Due to their versatility, lightweight nature, durability, resistance to corrosion, flexibility, and adept insulating characteristics, plastics have played a consequential role in societal development for over seventy years (Pan et al., 2023). As an illustration, from the commencement of its mass production around 1950 to the present, plastics have been used for the production of consumer goods, construction materials, vehicles, clothing, medical equipment, and electronics (Elizalde-Velázquez and Gómez-Oliván, 2021). Such has been the substantial reliance of industries spanning various sectors on plastics that research forecasts the annual production of plastics (390 million metric tonnes) (Zuri et al., 2023) to escalate twofold over the next two decades and experience a nearly fourfold surge by the year 2050 (Vitali et al., 2023). Nevertheless, it is crucial to acknowledge that despite the numerous practical applications of plastic, its extensive utilization has given rise to environmental concerns.

Recent data suggested that 76 % of the total plastic production is categorized as waste, of which 12 % undergo incineration, 79 % are buried or released into the environment, and only 9 % undergo recycling (Garcia and Robertson, 2017). This information holds significant importance, as it is known that plastic incineration and degradation in water and soil lead to the formation of microplastics and nanoplastics. Microplastics (MPs) are commonly defined as solid plastic particles that are insoluble in water and have dimensions of less than five millimeters (Kye et al., 2023). Meanwhile, nanoplastics are even smaller, measuring <1000 nm (Hartmann et al., 2019). Irrespective of their dimensions, MPs and nano plastics have been reported to be found across the atmosphere (Chen et al., 2020), soil (Yang et al., 2021), surface water (Fan et al., 2022), seafood (Unuofin and Igwaran, 2023), and other products intended for human consumption (Alak et al., 2022; Sewwandi et al., 2023). In surface water, concentrations of plastic particles have been observed to range from 5 to 34 particles per liter in Poyang Lake, China (Yuan et al., 2019), from 130 to 287 particles per liter in Campeche, Mexico (Hernandez et al., 2021), and approximately 10 to 100 particles per liter in the Province of Esmeraldas, Ecuador (Capparelli et al., 2021). Therefore, MPs and nanoplastics represent a significant threat to wildlife, as they have the potential to be consumed by diverse organisms, resulting in bioaccumulation and the disruption of entire food webs (Malafeev et al., 2023).

In an effort to minimize the occurrence and adverse consequences associated with MPs in the environment, certain governments have implemented prohibitions on the inclusion of plastic microbeads in cosmetics, personal care products, natural health products, and non-prescription drugs (Pettipas et al., 2016; Mitrano and Wohlleben, 2020; Ju et al., 2021a, 2021b). Furthermore, in various regions across Asia, Africa, Europe, North America, South America, and Oceania, no fewer than 30 countries have enacted partial or comprehensive restrictions on using single-use plastic bags (Dikgang et al., 2012; Bergmann et al., 2015; Ogunola et al., 2018). Nevertheless, these endeavors have proven insufficient, compelling the scientific community to discern sustainable and biodegradable alternatives that match exfoliating microplastics in terms of cost, mechanical properties, solvent resistance, smooth surface morphology, and uniform size. Three categories of biodegradable materials have been proposed as prospective alternatives to conventional plastics: natural hard materials (such as walnut shells and avocado seeds) (Shejkar et al., 2020; Martins et al., 2022), natural polymers (including chitosan, cellulose, alginate, lignin, and starch) (Gheorghita et al., 2020; Herrera-Vázquez et al., 2022; Namphonsane et al., 2023), and bio-based synthesized polymers (such as polycaprolactone and polylactic acid) (Delgado-Aguilar et al., 2020).

Chitosan, the deacetylated form of chitin, has garnered considerable attention as a structural biomaterial across various sectors, including food, medical, and cosmetic industries (Ju et al., 2021a, 2021b). It has emerged as a versatile material for food packaging production (Ashrafi et al., 2018; Cazón and Vázquez, 2019), the manufacturing of dressings and bandages (Dai et al., 2011; Verma et al., 2023; Zhao et al., 2023), drug delivery systems (Wei et al., 2020), biosensing devices (Kim et al., 2022), and environmental remediation endeavors (Issahaku et al., 2023), among other applications. Hence, this material stands as one of the most extensively researched biopolymers, scrutinized not solely for its chemical and physical attributes but also for its biocompatibility, biodegradability (Cazón and Vázquez, 2020; Hasan et al., 2020), and minimal toxicity (Kean and Thanou, 2010a, 2010b), rendering it a more sustainable alternative to conventional plastics. Chitosan degradation can ensue under environmental conditions involving biological and enzymatic processes and external factors such as temperature and humidity (Priyadarshi and Rhim, 2020). A study revealed that 93.2 % of chitosan spheres underwent degradation following one month of seawater immersion, whereas commercial polyethylene microspheres' degradation was negligible (Ju et al., 2021a, 2021b). Concurrently, all chitosan components within chitosan-polyethylene films, when exposed to open fields, experienced complete degradation, whereas the polyethylene films remained structurally intact throughout the incubation period (Makarios-Laham and Lee, 1995). In terms of toxicity, Opanasopit et al. (2007) found that lactic acid-chitosan salts, with a degree of deacetylation (DD) of 87 % and various molecular weights (20, 45, 200, and 460 kDa), demonstrated low cytotoxicity against Caco-2 cells. The IC50 values were 0.38, 0.31, 0.34, and 0.37 ± 0.08 mg/mL for each of the molecular weights tested. Similarly, Huang et al. (2004) observed comparable behavior in chitosan molecules with molecular weights ranging from 213 to 10 kDa and DD percentages from 88 % to 46 % when tested against A549 cells, with IC50 values ranging from 1.1 to 1.2 mg/L.

Despite extensive research into the toxicity of chitosan and its derivatives, the majority of studies have been conducted using cell lines. Therefore, there is a knowledge gap regarding the scope of this biopolymer in aquatic organisms. Herein, this research work aimed to (1) evaluate whether or not chitosan biopolymer films (CBPF) might impact the gut, gills, brain, and liver of *Danio rerio* adults and (2) compare those toxic effects against the ones induced by conventional MPs. As chitosan has been previously associated with antioxidant effects, it is suggested that CBPF will generate a non-severe toxic response in *Danio rerio* organs.

## 2. Method

### 2.1. Reagents

Fluorescent polystyrene and non-fluorescent polystyrene microplastics of 0.4–0.6 μm (CAS number: 9003-53-6) were acquired from Spherotech, headquartered in Lake Forest, Illinois. Bovine Gelatin with a

Bloom value of 290 was supplied by Duche® (Toluca, Mexico). Whey protein, sourced from the rennet cheese process, was acquired from Darigold Inc. (Seattle, WA, USA). Glycerol (98 % reagent grade) and lactic acid (85 %) were procured from J.T. Baker (Cd. Mexico, Mexico). Commercial-grade low molecular weight chitosan, with a molecular mass ranging from 50,000 to 190,000 Da and a degree of deacetylation exceeding 75 %, and all the remaining reagents were obtained from Sigma-Aldrich (Saint Louis, MO, USA).

### 2.2. Chitosan biopolymer films (CBPF)

#### 2.2.1. CBPF preparation

The CBPF were synthesized following the procedure outlined by Herrera-Vázquez et al. (2021). Briefly, a 1.5 % (*w/v*) chitosan solution was prepared by dissolving chitosan in distilled water at 70 °C, supplemented with 1 % (*v*/v) lactic acid. Subsequently, this solution was added with gelatin (5 %, w/v), whey protein (2.5 %, w/v), and glycerol (6 %, w/v). Glycerol served as a plasticizing agent. The film creation process began with gradually cooling the film-forming solution (FFS) under continuous stirring until it reached a temperature of 40 °C. Following this, 5 mL of the FFS was evenly poured into Petri dishes (5 cm in diameter) positioned on a flat surface to guarantee consistent thickness. Finally, all Petri dishes underwent a drying phase within a controlled chamber (ITH-75: Lumistell, Gto, Mexico) at a constant temperature of 30 °C for 48 h. For subsequent analysis, the CBPF samples were meticulously extracted from their molds, ground up, and sifted to achieve a particle size of 1 mm. Fluorescent CBPF was prepared following the previously outlined procedure. However, in this instance, the fluorescent coloring, Brilliant Blue FCF (Blue 1; Deimas, Puebla, Mexico), was integrated into the FFS after the dissolution of the polymers. It is paramount to stand out the food-grade dye was dissolved in a mixture of glycerol and water (50:50) at a temperature of 80 °C before its usage.

### 2.3. Confocal laser scanning microscopy

An inverted confocal laser scanning microscope (CLSM) model LSM 880 (Carl Zeiss, Germany) was employed for analyzing polystyrene beads (PB) lacking fluorescence and fluorescent beads (FB) exhibiting noticeable fluorescence at 488 nm. The observations were conducted on a 63 × 1.4 Zeiss Plan Apochromat oil-immersion DIC M27 objective. The imaging process involved a dual-channel approach, utilizing a 405 nm laser for fluorescence microscopy and light-transmitted microscopy for contrast enhancement. The captured images were standardized to a resolution of 2048 × 2048 pixels and saved in TIFF format. The determination of particle size for both PB and FB was accomplished through ImageJ software, version 1.47 (http://imagej.nih.gov; National Institute of Health, Bethesda, MD, USA). Each particle underwent measurement using the software's length tool, and the resultant data was employed for subsequent comparative analysis.

### 2.4. Atomic force microscopy (AFM)

An Innova Atomic Force Microscope (AFM) from Veeco Instruments Inc. (USA) was employed to assess and compare the dimensions of polystyrene beads (PB) and fluorescent beads (FB). Solutions containing the designated samples were meticulously applied onto glass slides and securely affixed through the precise application of carbon tape. Utilizing a DNP-10 tip and a scan rate of 1 Hz, 2D height images were acquired in contact mode and analyzed using NanoScope Analysis v1.4 software (Bruker, USA). For the image processing, a flattening at 1 order was applied, and manual adjustment of the data scale was performed per the color bars embedded within each image. All sample images were cropped within a 8.0 μm scan size, and the dimensions of each particle were determined using the sectioning tool integrated into the software interface.

### 2.5. Danio rerio upkeeping and exposure

Adult male and female *Danio rerio* (AB strain) were maintained in 100-l aquariums, ratio 1fish/L, filled with dechlorinated and UV-filtered water maintained at specific conditions (temperature: 27 ± 1.5 °C, pH: 7.2–7.6, with a light-dark cycle of 14:10). Water changes were conducted every three days, and the fish were fed twice daily with *Artemia salina naupli*. To maintain exposure conditions controlled, a total of 210 adult fish were distributed among seven separate systems. Each system consisted of 30 fish accommodated in 30 l of dechlorinated and UV-filtered water. Within this arrangement, one system served as the control group, while the remaining six systems were dedicated to subjecting the fish to varying concentrations of PB named MPs (25, 75, 100 particles/L) and CBPF (25, 75, 100 particles/L). The concentrations of MPs employed in this experiment encompass a range that has been documented to exist within surface waters on a global scale. The exposure spanned four months under consistent temperature and light-dark cycles, resembling the standard conditions for fish maintenance. Regular water replacement occurred every other day throughout the entire duration of the experiment for each system.

### 2.6. Euthanasia and fish dissection

Following the designated exposure period, no deceased fish were observed within the control group or the CBPF systems. Conversely, the experimental systems using PB revealed an average mortality rate of 2 fish (with a standard deviation of ±1). Consequently, twenty-seven fish were selected for subsequent analyses encompassing oxidative stress quantification, gene expression assessment, and histological examinations. Twelve fish were employed for each of the initial two tests. However, a reduced sample size was used for histological analysis, comprising only three fish for the examination process. All fish were euthanized through hypothermic shock. Subsequently, a precise longitudinal incision was made in the thoracic region using surgical scissors, followed by a meticulous dissection using dissecting forceps to extract the brain, liver, gills, and gut from each specimen. The extracted organs were transferred into Eppendorf tubes. Tubes used for oxidative stress quantification were filled with 1 mL of phosphate-buffered saline solution with a pH of 7.4. Conversely, tubes for gene expression evaluation and histopathological examinations were filled with RNALater (QIAGEN) and buffered formalin, respectively. These tubes were meticulously stored at a controlled temperature ranging from 2 °C to 4 °C until further analysis.

### 2.7. Oxidative stress evaluation

The evaluation of oxidative stress was carried out following the procedure outlined by Elizalde-Velázquez et al., 2023. Briefly, the tissue underwent homogenization using a rotor-stator homogenizer. Following homogenization, two separate tubes were generated from each sample. In the first tube, 300o μL of the homogenate was mixed with 20 % trichloroacetic acid and then centrifuged at 11495 rpm at 4.0 °C for 15 min. The resulting precipitate was utilized to measure the content of carbonylated proteins (PCC) using the methodology detailed by Levine et al. in 1994. Simultaneously, the supernatant was used to assess the extent of lipoperoxidation (LPX) and the hydroperoxides (HPC) levels following the procedures outlined by Buege and Aust in 1978 and Jiang et al. in 1992, respectively. In preparing the second tube, 700 μL of homogenate underwent centrifugation at 12,500 rpm at 4.0 °C for 15 min. The resulting supernatant was then employed to determine the activity of superoxide dismutase (SOD) and catalase (CAT), utilizing the methodologies described by Misra and Fridovich (1972) and Radi et al. (1991), respectively.

### 2.8. qPCR

Samples-thawing was meticulously executed in an ice bath. Subsequently, each tissue sample underwent the RNA isolation protocol utilizing the RNeasy Mini Kit from QIAGEN. The isolated RNA purity was assessed using spectrophotometry, employing a NanoDrop (model 2000/2000c, Thermo Scientific, USA). A sterile Eppendorf tube, free from RNases, served as the vessel for the initiation of reverse transcription. Within this tube, a solution was prepared by combining 2.0 μL of 7× gDNA Wipeout Buffer obtained from the QuantiTect Reverse Transcription Kit by QIAGEN, along with 10.0 μL of the RNA template and 2.0 μL of RNase-free water, also supplied in the QuantiTect Reverse Transcription Kit. Subsequently, the resulting mixture underwent incubation at 42 °C for 2 min, followed by prompt cooling on ice. After cooling the mixture, 1.0 μL Quantiscript reverse transcriptase, alongside 4.0 μL Quantiscript RT Buffer 5× and 1.0 μL of RT Primer Mix from the QuantiTect Reverse Transcription Kit, were added. The resultant combination underwent an initial incubation phase at a temperature of 42 °C for 15 s, succeeded by a subsequent incubation at 93 °C for 3 min. This sequential process enabled the deactivation of reverse transcription. The qPCR reaction was conducted using 25 μL of the 2× QuantiTect SYBR Green PCR (QIAGEN), along with 1.0 μL of each primer (Table 1), 4.0 μL of cDNA, and 19 μL of RNase-free water, combined accordingly. The thermal cycling program included an initial denaturation step at 94 °C for 10 min, followed by 35 cycles of denaturation at 94 °C for 15 s, primer annealing for 30 s, and extension at 72 °C for 30 s. The qPCR apparatus utilized for this experiment was the Gene Q Rotor from QIAGEN. To standardize the expression levels of target genes, the β-actin gene was employed. The quantification of mRNA expression alterations was done using the $2- \Delta \Delta Cq$ method, as outlined by Pfaffl in 2001, Pfaffl et al. in 2002, and Schmittgen and Livak in 2008. After the qPCR amplification cycles finished, an analysis of the dissociation curve was initiated using these parameters: an initial denaturation phase at 95 °C for 10 s, a decrease to 65 °C for 10 s, then a gradual increase back to 95 °C for 10 s, increasing by 0.2 °C increments. This rigorous protocol was employed to distinguish specific products from non-specific ones within the samples. Data points were systematically collected at each increment of the melting curve. To validate the results, negative controls were integrated, utilizing samples lacking a template, with RNase-free water serving as the substitute.

### 2.9. Histological analysis

Following 48 h of fixation in formalin, the samples were embedded in CRYO GLUE and underwent freezing at −27 °C. Subsequently, after a 2-h interval, cross sections (50 μm) of the organisms' gill, digestive tract, brain, and liver were generated using a cryostat microtome (CM1850, LEICA, USA). All organs were then scrutinized using a confocal microscope (LSM 880, Carl Zeiss, Germany) equipped with three lasers emitting at 405, 488, and 561 nm wavelengths. The laser emission was selected based on the autofluorescence presented in the samples using the lambda mode, enabling a spectral range from 400 to 700 nm to be obtained (Hernández-Varela et al., 2022). The images were obtained using a 5× APO calibration objective and RGB images of 2048 × 2048 pixels were analyzed using the Zen 3.7.3 (blue edition, Carls Zeiss, Germany).

**Table 1**
Nucleotide sequences of the primers designed for the (qPCR) analysis.

| Gen | Access Number | Forward, Reverse | Primer Sequence (5′ → 3′) |
|---|---|---|---|
| *casp3* | NM_131877.3 | F | GATGAACGGAGACTGTGTGG |
| | | R | CTGAAGGCATGGGATTGAGG |
| *casp9* | NM001007404 | F | CGG AGG AGG TGA GAA GGA TAT |
| | | R | TCC AGC ACA GAT CAA GAT T |
| *bax* | AF231015 | F | GGC TAT TTC AAC CAG GGT TCC |
| | | R | TGC GAA TCA CCA ATG CTG T |
| *bcl2* | NM_001030253 | F | TAC GGG ATG CTG GAG ATG AA |
| | | R | CCC AGT TCA CTC CGT CTC TA |
| *p53* | NM_001271820 | F | GCG GAT TTG CTT TGT GGA TG |
| | | R | CCG ACC TCC TCT CCA CTA AA |
| *nrf1* | NM_001328540.1 | F | CAG TGA CAG TAG CCC AGG TG |
| | | R | CTG ACG CTT GTG TGG TTT GG |
| *nrf2* | NM_182889.1 | F | GGC GAT CCT CCT GTA AAC CC |
| | | R | CCG AAG GAT CCG TCT TCG GT |

### 2.10. Integrated biomarker response (IBR) index

The analysis of oxidative stress data employed the "Integrated Biomarker Response (IBR) Index" methodology proposed by Sanchez et al. (2013), which, as its name says, enables the integration of multiple biomarker responses. In this method, biomarkers from each treatment group (Xi) were compared to those of the control group (Xo). The Xi/Xo ratio underwent logarithmic transformation (Yi) to mitigate variance. Subsequently, Yi values were standardized using the formula $Zi = (Yi-\mu)/s$, where μ and s denote the mean and standard deviation of Yi, respectively. The biomarker deviation index (A) was calculated as the discrepancy between Zi and Z0. Subsequently, A values were represented in a star plot to illustrate the integrated biomarker responses. Moreover, the absolute values of A for each biomarker were aggregated to compute the IBR values.

### 2.11. Statistical analysis

Homoscedasticity was verified using Bartlett tests, and normality was assessed using the Shapiro-Wilk test. Mean differences were evaluated using the Tukey test, with a significance threshold established at $p < 0.05$. To explore variances among treatment groups, a one-way ANOVA test was conducted at a significance level of $\alpha = 0.05$, employing Sigma Plot 12.3 software. The outcomes of all experiments were reported as the mean ± standard deviation (SD). The data obtained from histological analysis were transferred from a data sheet to the statistical software package SPSS for processing. Subsequently, the Odds Ratio (OR) was computed, accompanied by its corresponding 95 % confidence interval (CI = 95 %). Likewise, a Pearson correlation analysis was performed to evaluate the association's strength between oxidative stress and gene expression outcomes, with a significance level set at $p < 0.05$. Additionally, the resultant correlation was visually represented using a heat map.

## 3. Results

### 3.1. MPs visualization

The CLSM data disclosed that the mean diameter of polystyrene and fluorescent beads was 0.494 ± 0.056 and 0.531 ± 0.045 μm, respectively (Fig. 1). In contrast to CLSM, AFM outcomes indicated that the mean diameter of non-fluorescent and fluorescent beads was 0.488 ± 0.042 and 0.512 ± 0.030 μm, respectively. Overall, the reported diameters of the MPs by the manufacturer align consistently with the dimensions elucidated in this investigation.

### 3.2. Oxidative stress

All organs exposed to MPs and CBPF showed either an increase or reduction in all oxidative stress biomarkers evaluated. Nevertheless, it is paramount to note that the responses varied among organs, treatments, and concentrations. For example, when comparing treatments, star plots illustrate a predisposition of MPs towards biomarkers indicative of oxidative damage (LPX, HPC, and PCC) (Fig. 2. I – IV). Meanwhile, the trend observed with CBPF leans towards activating antioxidant enzymes (SOD and CAT), which agrees with the well-established antioxidative

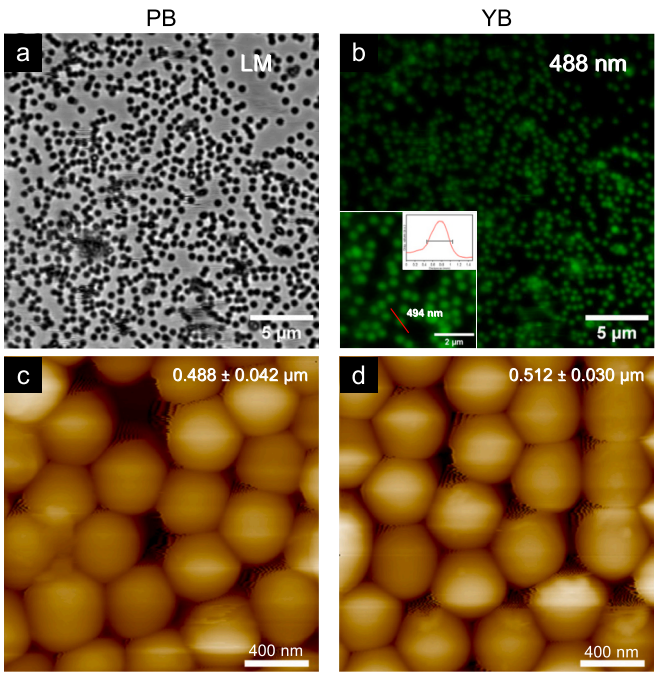


**Fig. 1.** CLSM images for polystyrene beads (PB) and fluorescent beads (FB), using a light-transmitted microscope (a) and a laser of 488 nm (b). AFM images for PB (c) and FB (d) were used to calculated the mean size of the particles show as inset.

properties found in chitosan. Regarding the organs examined, our findings indicate that the gut was the most adversely impacted by MPs, followed by the gills, brain, and liver. This finding is supported by the clear trend towards elevated levels of oxidative damage biomarkers in the organs showing the most significant impairment. While CBPF exhibited increased activity of antioxidant enzymes across all organs, there is a noticeable decrease in the levels of SOD and CAT in the gills and liver. Thus, it is believed these were the most affected organs by CBPF. Finally, as illustrated in Fig. 2, there is a notable increase in all oxidative stress biomarkers in a concentration-dependent manner compared to the control group. This elevation is corroborated by the escalating IBR values observed with higher concentrations of MPs and CBPF. However, an exception to this concentration-dependent trend is observed in the brain and liver with MPs, where IBR values decrease at 75 and 100 particles/L. The respective reductions in CAT and SOD could potentially elucidate this phenomenon.

### 3.3. Gene expression

As in oxidative stress, the expression of all genes underwent significant modifications in all treatments compared to the control group. Nevertheless, these alterations in gene expression were more pronounced in the case of MPs than CBPF. For instance, the heat maps' coloration (Fig. 3. I–IV) demonstrated lighter hues across all concentrations of MPs in almost all genes, but nrf1 and nrf2, signifying a more substantial up-regulation in gene expression. Besides the difference between treatments, a notable difference was observed in the expression levels of all genes across various organs. As an illustration, after exposure to microplastics (MPs), the gut exhibited the most pronounced elevation in the expression levels of p53, casp3, and casp9, in succession by the gills, liver, and brain. Conversely, in the context of exposure to CBPF, the gills demonstrated the most conspicuous escalation in the expression levels of casp3, casp9, and bax, followed in sequence by the gut, liver, and brain. Overall, the organs of fish exposed to MPs demonstrated the highest overexpression of the genes bax and p53, whereas those exposed to CBPF exhibited heightened expression of nrf1 and nrf2. Nevertheless, it merits attention to highlight that CPBF elicited the upregulation of apoptotic genes across all concentrations and in all organs examined. Ultimately, it is noteworthy to highlight that substantial differences in gene expression between concentrations were observed in fish exposed to MPs; however, such differences were not so evident in those exposed to CBPF.

### 3.4. Histological analysis

Although tissue analysis encompassed the examination of gills, gut, brain, and liver, it is imperative to underscore that the latter two organs did not manifest either the presence of MPs or any discernible tissue damage. Hence, only gills (Zone 1) and gut (Zone 2) were used to explain the changes related to the presence of microplastics (MPs), chitosan biopolymeric film (CBPF), and concurrent tissue damage. Furthermore, it is noteworthy that none of the organs in fish exposed to the control and CBPF exhibited the presence of either plastic and biopolymer particles or noticeable tissue damage. Regarding the organs demonstrating the presence of MPs, Fig. 4 distinctly illustrates the occurrence of plastic particles in the upper region of the primary gill lamellae (located below the operculum) in fish exposed to 75 and 100 particles per liter. In this context, it is noteworthy to emphasize that the incidence of MPs in gills led to significant tissue damage, including lamellae fusion (LF), erythrocyte infiltration (EI), and hemorrhage (H). Similar to the observations in the gills, Fig. 5 illustrates the presence of MP clusters in the intestines of fish exposed to all concentrations of polystyrene particles. Likewise, observations indicated that MPs caused notable tissue damage in this organ, denoted by hemorrhaging (H) and inflammatory cells (IC).

### 3.5. Pearson correlation

The heat maps presented in Fig. 6 visually depict the Pearson correlation between outcomes associated with oxidative stress and gene expression. Across all organs, the overall relationship between oxidative damage biomarkers and the expression of genes related to apoptosis, except for bcl2, manifests as positive and robust. Conversely, bcl2 demonstrates a compelling and positive correlation with the antioxidant enzyme activity of SOD and CAT, along with the expression of nrf1 and nrf2. Notably, the gills exhibit the most pronounced correlation among all variables, followed by the gut, liver, and brain.

### 3.6. Univariate analysis

The Odds Ratio (OR) serves as a metric employed to quantitatively assess the magnitude and directionality of the association between a specific risk factor or exposure and the probability of a distinct outcome. A value of the odds ratio exceeding 1 signifies an elevated likelihood of the event in the exposed group, indicative of a positive correlation with the given exposure. Conversely, an odds ratio below 1 implies diminished odds of the event in the exposed group, suggesting a potential protective influence. In the context presented herein, where the odds ratio surpasses 1 (Table 2), it can be deduced that the presence of MPs (microplastics) in the gut and gills positively correlates with the histological damage observed in those organs.

## 4. Discussion

Even though the inclination to innovate and devise eco-friendly alternatives to conventional plastics has risen in the last decade, none of the emerging biopolymer options have proven less toxic than traditional plastics when released into the environment. Until now, studies have predominantly focused on assessing the biodegradability of these biopolymeric alternatives compared to conventional plastics, leaving much unexplored territory regarding their overall environmental impact. In light of the preceding, this study aimed to assess and juxtapose the potential toxic effects that CBPF and polystyrene MPs may exert on *Danio*

# I) Gut

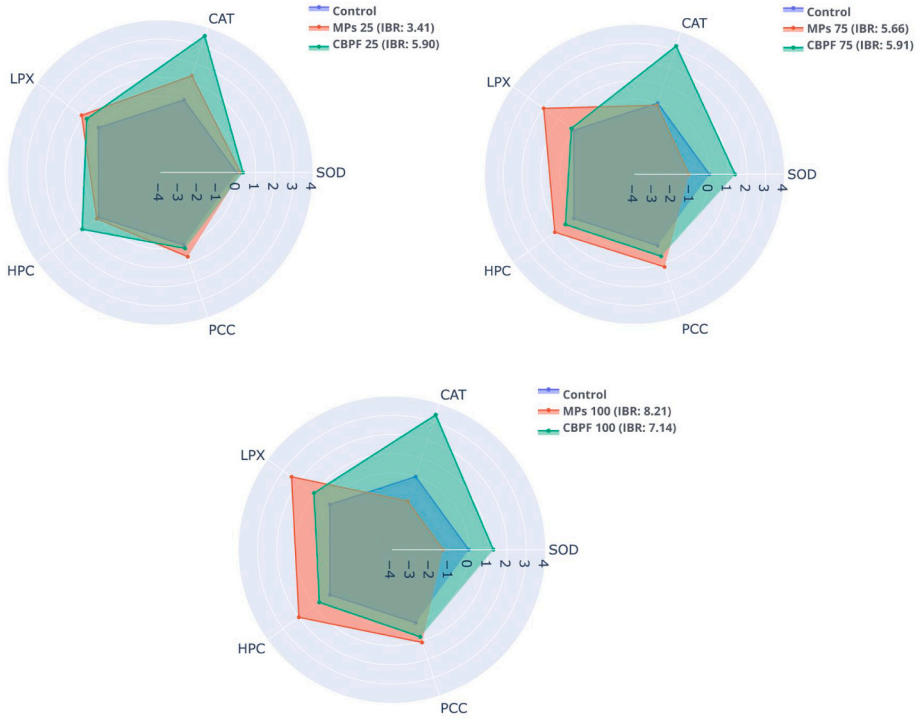


# II) Gills

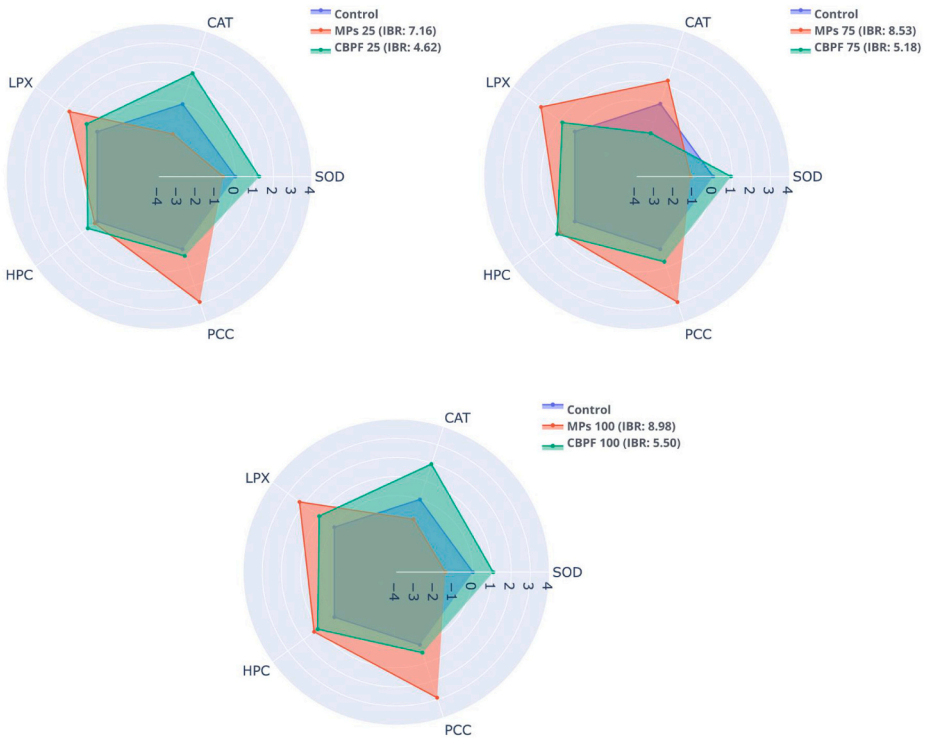


**Fig. 2.** Star plots of oxidative stress response of *Danio rerio* adults exposed to MPs (25, 75, and 100 particles/L) and CBPF (25, 75, and 100 particles/L). A comparative analysis was undertaken to assess the biomarkers (lipoperoxidation (LPX), hydroperoxides (HPC), carbonylated protein content (PCC), superoxide dismutase (SOD), and catalase (CAT)) observed in both the treatment and control groups. Regions above zero denote biomarker production, whereas areas below zero signify biomarker reduction. The numerical annotations delineate the oxidative stress responses identified in distinct organs: I) Gut, II) Gills, III) Brain, and IV) Liver.

# III) Brain

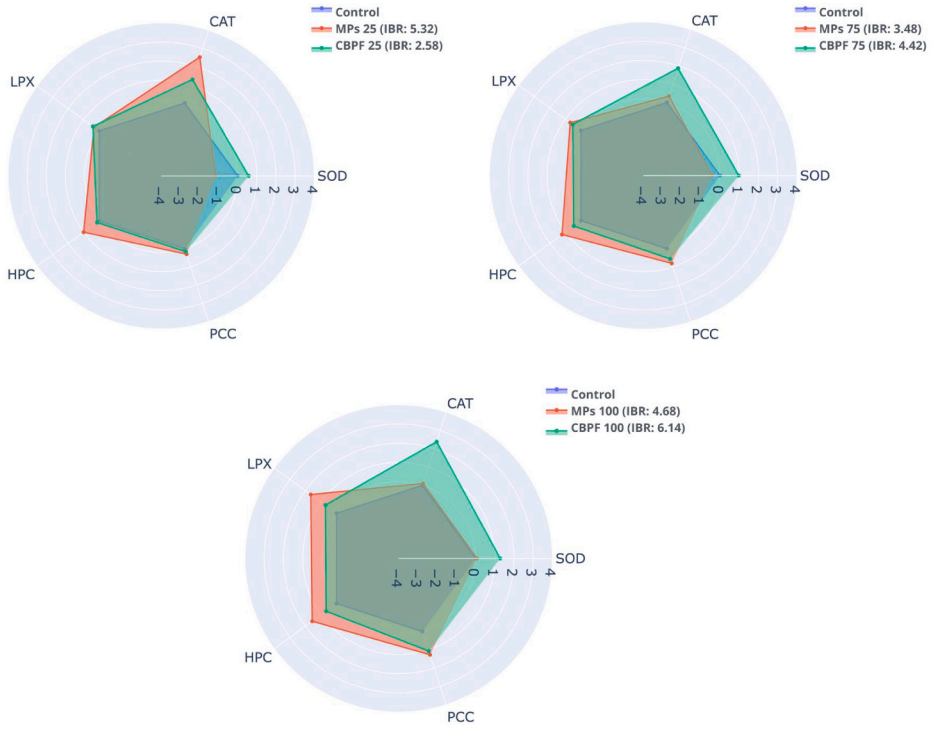


# IV) Liver

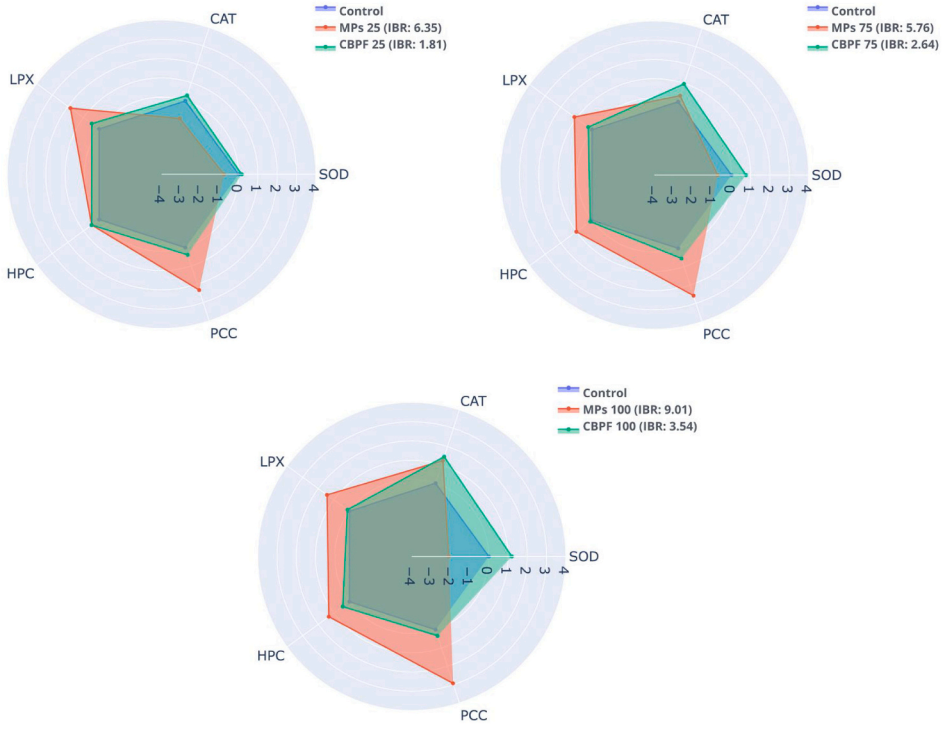


**Fig. 2.** (*continued*).

*rerio*'s organs following acute exposure (Van Roijen and Miller, 2022; Emadian et al., 2017). Based on our findings, it was observed that CBPF and MPs induced changes in the oxidative status of fish across various organs, including the gills, gut, brain, and liver. These outcomes are consistent with the findings reported by Wang et al. (2019), wherein exposure to 10 μm polystyrene MPs (2, 20, and 200 μg/L) for 60 days resulted in oxidative stress in the gill, intestine, and liver of *Oryzias melastigma*. In a corresponding manner, Usman et al. (2021)

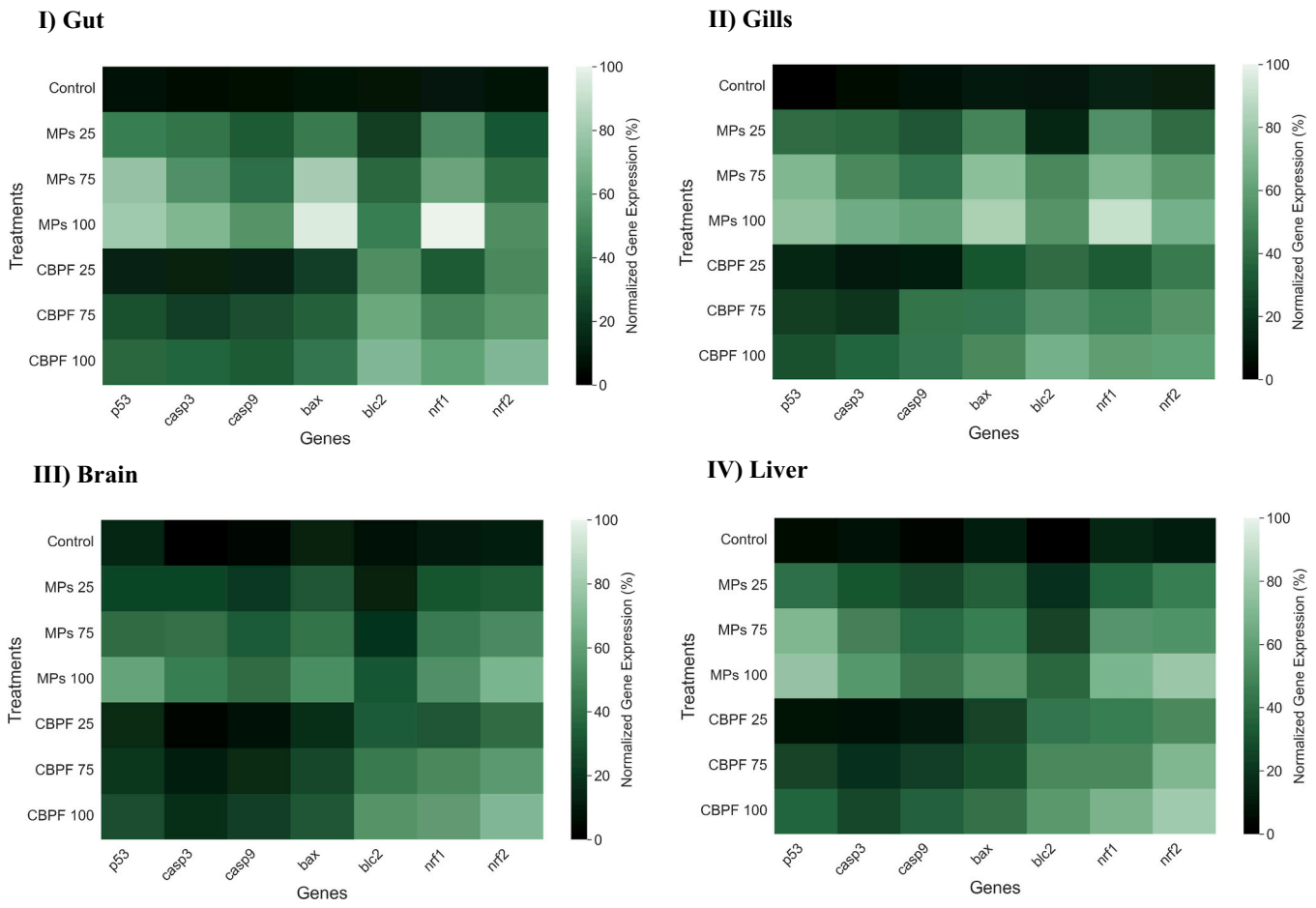


**Fig. 3.** Gene expression of *Danio rerio* adults exposed to MPs (25, 75, and 100 particles/L) and CBPF (25, 75, and 100/particles/L). The numerical annotations signify the gene expression levels observed in specific anatomical organs: I) Gut, II) Gills, III) Brain, and IV) Liver.

substantiated that the protracted exposure (21 d) of *Oryzias javanicus* to PS-MPs beads measuring 5.0 μm elicited oxidative stress in the cerebral and intestinal tissues. Additionally, in two recent studies conducted by Chen et al. (2022) and Cui et al. (2023), it was demonstrated that polystyrene MPs with sizes of 10 nm and 8.0 μm, at concentrations of 30 μg/L and 1000 ng/L, respectively, induced oxidative stress in the gills, kidney, liver, and muscles of *Ctenopharyngodon idellus* and *Cyprinus carpio*. It is crucial to highlight that the oxidative stress responses differed between the studies. Specifically, the 10 nm polystyrene MPs significantly increased the activities of superoxide dismutase (SOD) and peroxidase (POD). Conversely, the 8.0 μm polystyrene MPs reduced the activities of catalase (CAT), glutathione peroxidase (GSH-PX), and SOD while concurrently promoting the production of reactive oxygen species (ROS). Herein, 0.4 to 0.6 μm PS-MPs significantly enhanced the antioxidant activity of superoxide dismutase (SOD) and catalase (CAT), along with an augmentation in reactive oxygen species (ROS) production. The above discrepancies can be explained by the phenomenon called the toxic excitatory effect. Some authors, for instance, have mentioned that the activity of SOD and CAT tend to increase in reaction to a stress response imposed on organisms (Colín-García et al., 2023; Lee et al., 2023; Gutiérrez-Noya et al., 2023). Nevertheless, when this stress response surpasses a specific threshold, it may lead to the inhibition of antioxidant enzyme activity and the regulation of reactive oxygen species (ROS) metabolism in fish (Elizalde-Velázquez et al., 2022). Likewise, it is paramount to point out that variations in the observed oxidative stress responses could also be attributed to the distinct physiological functions of the assessed organs, along with the varying sensitivities exhibited by each tested organism.

Unlike MPs, CBPF showed a more substantial antioxidant response, which, as mentioned above, could be attributed to chitosan's inherent antioxidant activity. Previously, some authors have posited that the hydroxyl and amine functional groups within the chitosan molecule exhibit free radical scavenging properties (Park et al., 2004; Park et al., 2010). Likewise, other researchers have suggested substituting these functional groups diminishes the antioxidant efficacy (Anraku et al., 2008). Consequently, chitosan with a higher degree of deacetylation would manifest more remarkable radical scavenging capabilities. Besides the degree of deacetylation, it is crucial to consider the molecular weight of this molecule. Typically, chitosan demonstrates significant N2–O6 and O3–O5 hydrogen bonding interactions. However, high molecular weight (HMW) chitosan exhibits dense structures, enhancing the strength of intra-molecular hydrogen bonds and consequently diminishing the reactivity of hydroxyl and amino groups. This reduction in reactivity is anticipated to lower its antioxidant activity correspondingly (Anraku et al., 2018). Conversely, low molecular weight (LMW) chitosan possesses even denser structures, leading to decreased effectiveness of intra-molecular hydrogen bonding interactions. Corroborating the findings above, Chien et al. (2007) observed a diminishing trend in the antioxidant efficacy of chitosan with increasing molecular weights of 12.0, 95.0, and 318.0 kDa. Additionally, Li et al. (2022) exhibited elevated activities of SOD, CAT, and glutathione peroxidase (GPX) in juvenile yellow catfish that were fed a diet containing chitosan with a molecular weight of 39 kDa and a deacetylation degree of 93.7 %. In this study, the chitosan utilized possessed a molecular weight exceeding 50 kDa and a deacetylation degree surpassing 75 %, potentially accounting for the low toxic response observed in specific organs such as the gut and gills.

Up to date, the mechanism underlying the induction of reactive

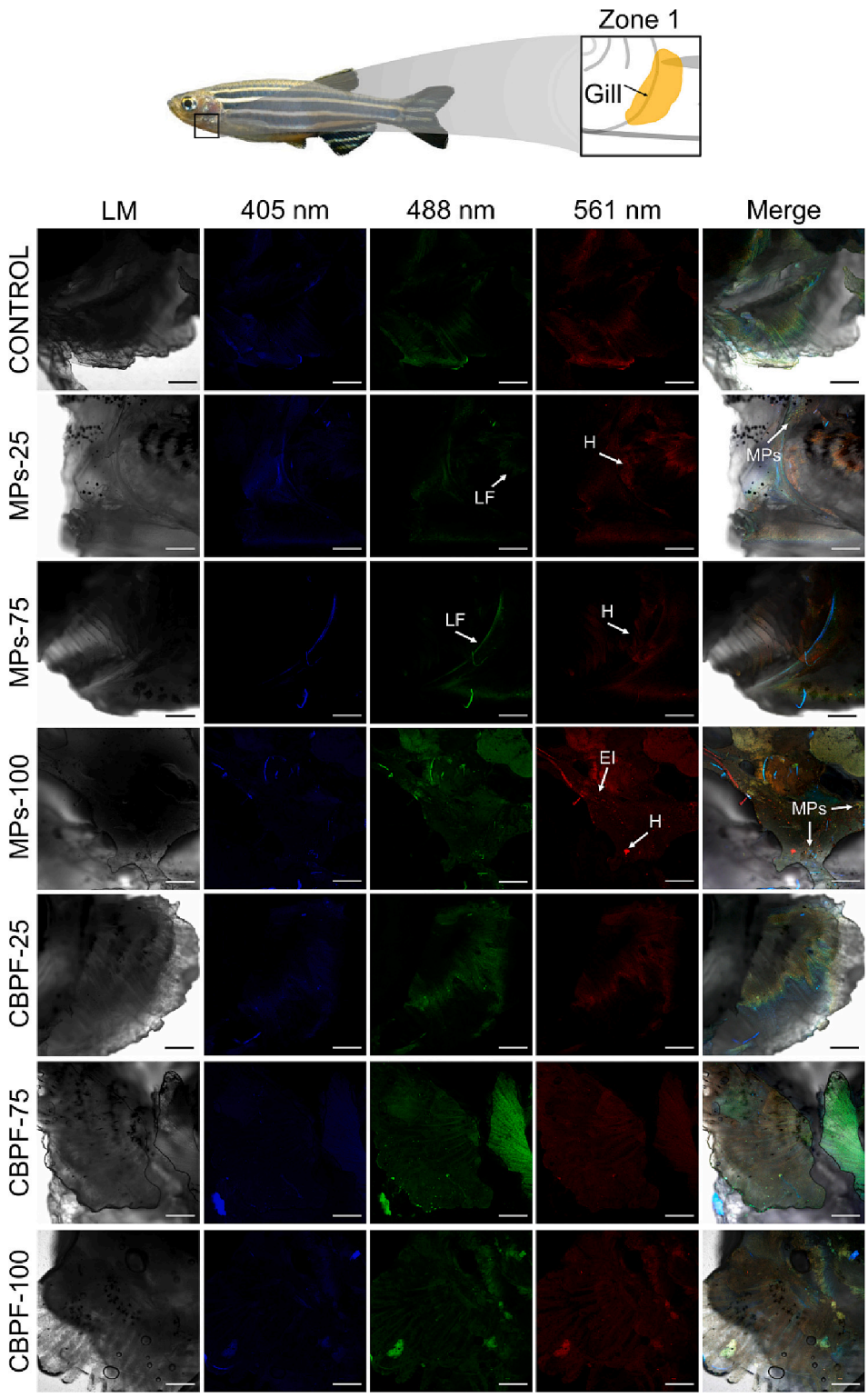


**Fig. 4.** Confocal microscopy images of *Danio rerio* gills (zone 1) exposed to MPs and CBPF at different concentrations (25, 75, and 100 particles/L). Arrows serve to denote the presence of MPs and concurrent tissue damage. H: hemorrhage. LF: lamella fusion. EI: erythrocyte infiltration. LM: light microscopy. MPs: microplastics. CBPF: chitosan biopolymeric films. Scale bar = 500 μm.

oxygen species (ROS) production by polystyrene MPs remains poorly understood. However, some recent studies have proposed that polystyrene MPs may induce ROS production through mitochondrial disruption. Meng et al., 2022 and Das (2023), for instance, highlighted that MPs can accumulate within mitochondria, resulting in membrane damage and disruption of the electron transport chain. Nonetheless, other authors have pinpointed that MPs might alter cellular processes related to oxygen supply, consumption, or ion exchange (Yin et al., 2018; Shang et al., 2021; Elizalde-Velázquez et al., 2022). Therefore, it is also plausible that these disruptions could contribute to an oxidative stress environment, potentially leading to ROS production. In any case, the heightened intracellular reactive oxygen species (ROS) levels

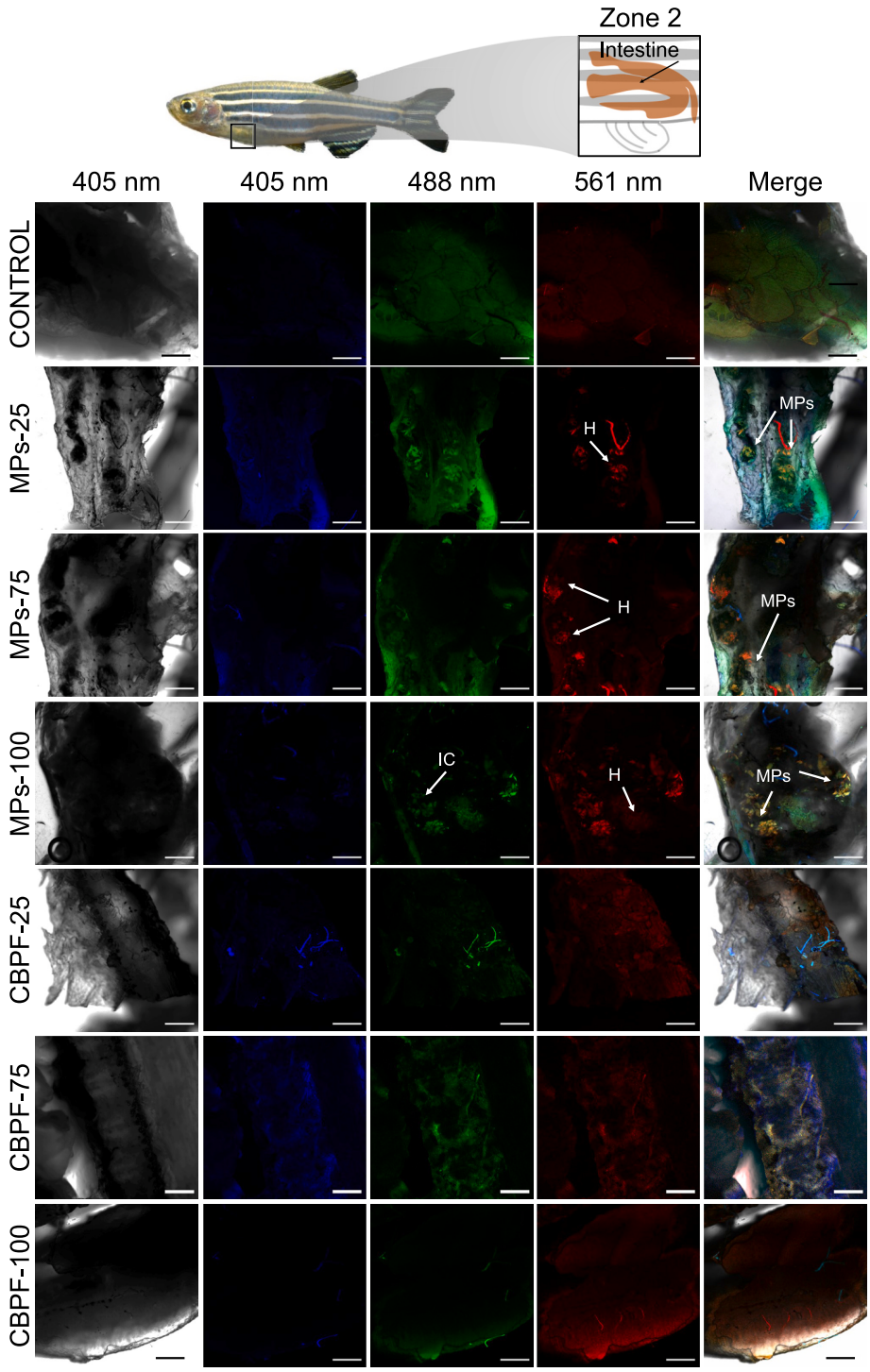


**Fig. 5.** Confocal microscopy images of *Danio rerio* gut (zone 2) exposed to MPs and CBPF at different concentrations (25, 75, and 100 particles/L). Arrows serve to denote the presence of MPs and concurrent tissue damage. H: hemorrhage. IC: inflammatory cells. LM: light microscopy. MPs: microplastics. CBPF: chitosan biopolymeric films. Scale bar = 500 μm.

generated by MPs can activate signal transductions facilitated by mitogen-activated protein kinase (MAPK), thereby fostering the expression of genes associated with antioxidant and apoptotic responses. For example, Jeong et al., 2017 demonstrated that polystyrene MPs activated signal transduction pathways of p38 and p-EKR, both members of the MAPK family, leading to a final augmented expression of the nrf2 gene. In addition, Hu et al., 2021 pointed out that polystyrene MPs trigger the activation of the p38 MAPK signaling pathway, ultimately resulting in the induction of cellular apoptosis. The findings above align with the results presented in this study, wherein the exposure of adult *Danio rerio* to polystyrene MPs led to heightened expression of genes associated with antioxidant (nrf1 and nrf2) and apoptotic responses (caps3, casp9, p53, bax, and bcl2) across all organs (Fig. 3 I – IV). Despite CPBF also prompting the expression of apoptotic-related genes, it is remarkable to indicate this expression was not significantly different from the control group in all organs evaluated. However, a distinct pattern was observed for the nrf1 and nrf2 genes, as their expression demonstrated a significant up-regulation following exposure to CPBF. As

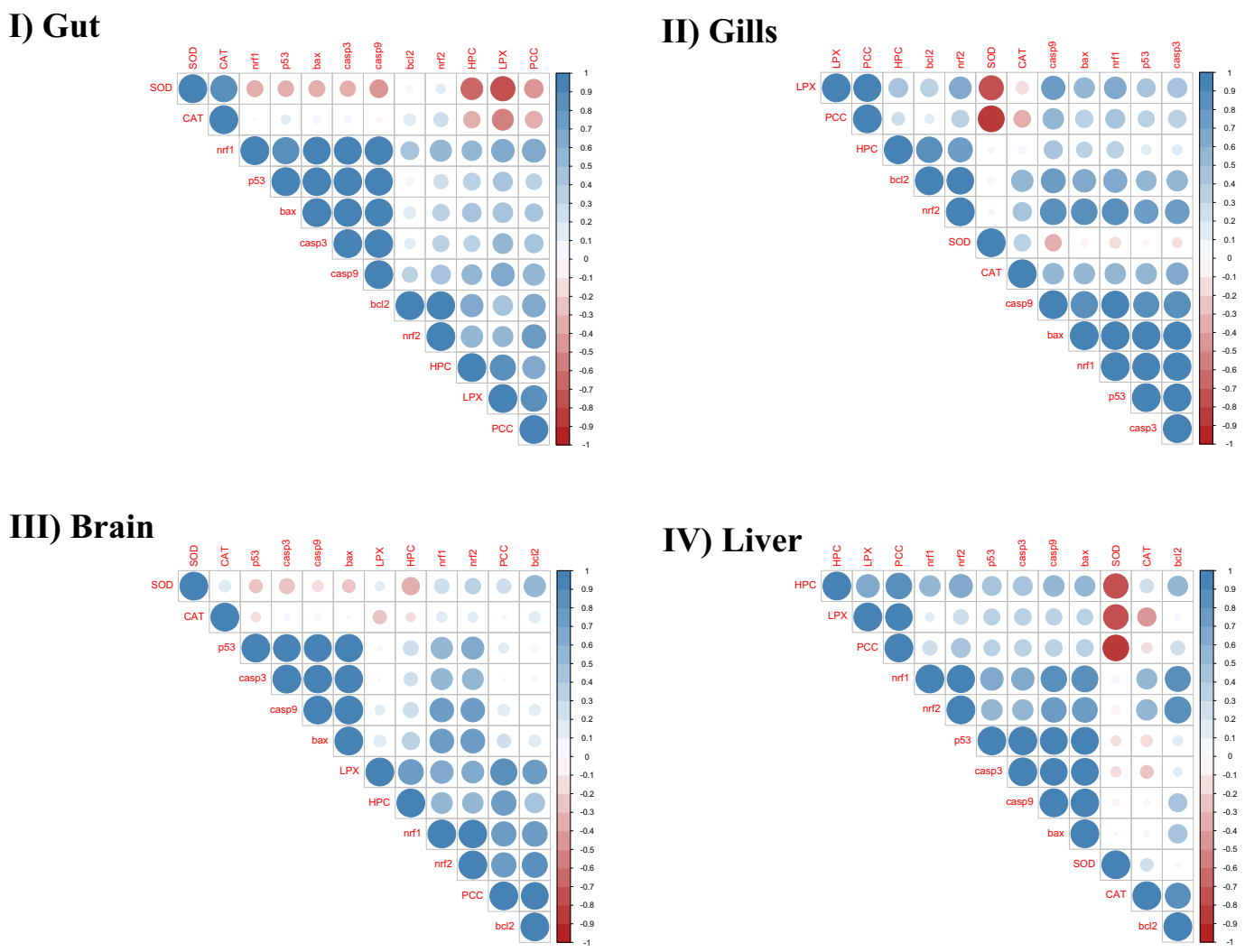


**Fig. 6.** Pearson correlation of each organ: I) Gut, II) Gills, III) Brain, and IV) Liver.

**Table 2**
Odds ratios (OR) for the risk associated with histological damage in both the intestine and gills attributable to microplastics (MPs).

| Tissue | Treatment | | Histological damage | | | |
|---|---|---|---|---|---|---|
| | | | % | OR | IC95% (OR) | p |
| Gills | Control | No | 100 | – | – | – |
| | | Si | 0.0 | 1.00 | – | – |
| | MPs | No | 48.9 | – | – | – |
| | | Si | 51.1 | **2.04** | **1.51–2.75** | **<0.0001** |
| | CBPF | No | 100 | – | – | – |
| | | Si | 0.0 | – | – | – |
| Gut | Control | No | 100 | – | – | – |
| | | Si | 0.0 | 1.00 | – | – |
| | MPs | No | 31.1 | – | – | – |
| | | Si | 68.9 | **3.21** | **2.08–4.96** | **<0.0001** |
| | CBPF | No | 100 | – | – | – |
| | | Si | 0.0 | – | – | – |

mentioned above, this observation could be elucidated by the extensively documented antioxidant properties associated with chitosan (Abd El-Hack et al., 2020). In agreement with the above, Yan et al., 2017 demonstrated the expression levels of SOD, CAT, and GPX increased after being fed with chitosan.

MPs not only induced oxidative stress and triggered the up-regulation of apoptotic genes but also caused tissue damage in the gills and gut. Overall, this damage could be attributed to either the overproduction of reactive oxygen species (ROS) in those organs or the simple presence of MPs. ROS can be generated by cells as a defense mechanism against pathogens or as byproducts of regular cellular metabolism (Canton et al., 2021). Nevertheless, when the production of ROS is not carefully controlled, it has the potential to cause tissue damage and trigger inflammation (Yang and Lian, 2020). Herein, our OR indicated that histological damage is mainly attributed to MP incidence. This finding is noticeable as previous results have also suggested that polystyrene spheres and chitosan might cause substantial damage to the gills and gut. For instance, Wang et al., 2019 showed polystyrene MPs produced a loose arrangement of gill filaments, a disintegration in the apical region of gill filaments, and a shortening and thickening of gill lamella in marine medaka after 60 days of exposure. Likewise, a study carried out by Jin et al., 2018 demonstrated that polystyrene MPs prompted significant increases in the volume of mucus in the gut of zebrafish after 14 days. The tissue alterations described earlier, along with those documented in this research, are of utmost importance to organisms, as they could potentially lead to adverse effects in the affected organs. To illustrate, gills serve as vital organs for respiratory and osmoregulatory functions. Consequently, inhaling polystyrene microspheres into fish's gills can induce transient changes in oxygen consumption and ion regulation, ultimately leading to compromised metabolic efficiency, impaired cellular functions, and systemic stress responses. Concerning CBPF, no presence of the particles was observed

in any organ, and there were no indications of induced tissue alterations. This absence of tissue damage may be attributed to either the substantial size of the particles employed in this study or the fish's effective degradation of the particles. Chitosan degradation in vertebrates is primarily attributed to the enzymatic action of lysozyme and bacterial enzymes within the colon (Kean and Thanou, 2011). However, it is noteworthy that eight chitinases belonging to the glycoside hydrolase 18 family exist in humans, three of which have demonstrated enzymatic capability (Funkhouser and Aronson, 2007). Chitinases are enzymatic proteins that catalyze the hydrolysis of β-1,4-linked *N*-acetyl-d-glucosamine (GlcNAc) bonds present in chitin and its derivatives (Teng et al. (2014)). These enzymes, alongside lysozyme, are also detected in *Danio rerio* (Teng et al., 2014; Chen et al., 2022). For example, Teng et al. (2014) reported the expression of the chitinase-3 gene Chi3 in zebrafish's liver and gut, indicating its potential capacity to hydrolyze chitin. Likewise, it is noteworthy that the rate and extent of chitosan biodegradation within living organisms are contingent upon the degree of deacetylation (DD). Higher degrees of deacetylation tend to lower the degradation rate (Yang et al., 2007; Kean and Thanou, 2010a, 2010b). Herein, it is likely that, given adequate time and appropriate conditions, the chitosan would have degraded sufficiently for consequent excretion.

## 5. Conclusions

The study found no evidence of severe toxic effects induced by CBPF tested in this study (1 mm size). Overall, CBPF denoted a low toxic response compared to MPs. However, the researchers express interest in exploring the impact of these biopolymer films on other organisms, given the varying toxic responses observed with microplastics (MPs) in different species. Also, it is proposed that a food-chain simulation rather than individual organism exposure be conducted. This approach accounts for particle degradation, alterations in size, structure, surface chemistry, morphology, and the transfer of contaminants from one organism to another, potentially resulting in varied toxic responses. In addtition to the above, the authors suggest investigating whether CBPF can induce toxic effects by manipulating the particle size. The study used 1 mm particles, raising concerns about potential translocation within fish organs. To address this, the authors propose experimenting with different particle sizes, considering that varying sizes might influence the toxic response of CBPF. The authors emphasize the importance of particle size and form in determining toxicity. It is worth noting that the study exclusively exposed fish to CBPF beads, but in the environment, biopolymer films can degrade in various ways, resulting in different particle forms. Consequently, the authors believe that using alternative forms of CBPF for organism exposure could yield valuable insights, prompting the need to document and compare the differences in toxic effects.

## CRediT authorship contribution statement

**Selene Elizabeth Herrera-Vázquez:** Methodology, Formal analysis, Data curation, Conceptualization. **Gustavo Axel Elizalde-Velázquez:** Writing – original draft, Methodology, Investigation, Formal analysis, Data curation, Conceptualization. **Leobardo Manuel Gómez-Oliván:** Writing – review & editing, Writing – original draft, Visualization, Supervision, Resources, Investigation, Funding acquisition, Formal analysis, Conceptualization. **José Jorge Chanona-Pérez:** Supervision, Software, Formal analysis. **Josué David Hernández-Varela:** Software, Formal analysis, Data curation. **Misael Hernández-Díaz:** Validation, Software, Methodology, Data curation. **Sandra García-Medina:** Software, Methodology, Investigation, Formal analysis. **José Manuel Orozco-Hernández:** Validation, Software, Methodology, Formal analysis. **Karla Colín-García:** Methodology, Data curation.

## Declaration of competing interest

The authors declare that they have no known competing financial interests or personal relationships that could have appeared to influence the work reported in this paper.

## Data availability

Data will be made available on request.

## Acknowledgments

This study was made possible by financial support the Consejo Nacional de Ciencia y Tecnología (CONACyt, Project 300727).

## References

Abd El-Hack, M.E., El-Saadony, M.T., Shafi, M.E., Zabermawi, N.M., Arif, M., Batiha, G. E., Al-Sagheer, A.A., 2020. Antimicrobial and antioxidant properties of chitosan and its derivatives and their applications: a review. Int. J. Biol. Macromol. 164, 2726–2744.

Alak, G., Uçar, A., Parlak, V., Atamanalp, M., 2022. Identification, characterisation of microplastic and their effects on aquatic organisms. Chem. Ecol. 38 (10), 967–987.

Anraku, M., Kabashima, M., Namura, H., Maruyama, T., Otagiri, M., Gebicki, J.M., Tomida, H., 2008. Antioxidant protection of human serum albumin by chitosan. Int. J. Biol. Macromol. 43 (2), 159–164.

Anraku, M., Gebicki, J.M., Iohara, D., Tomida, H., Uekama, K., Maruyama, T., Otagiri, M., 2018. Antioxidant activities of chitosans and its derivatives in in vitro and in vivo studies. Carbohydr. Polym. 199, 141–149.

Ashrafi, A., Jokar, M., Nafchi, A.M., 2018. Preparation and characterization of biocomposite film based on chitosan and kombucha tea as active food packaging. Int. J. Biol. Macromol. 108, 444–454.

Bergmann, M., Gutow, L., Klages, M., 2015. Marine Anthropogenic Litter. Springer Nature, p. 447.

Buege, J.A., Aust, S.D., 1978. Microsomal lipid peroxidation. Methods Enzymol. 52, 302–310.

Canton, M., Sánchez-Rodríguez, R., Spera, I., Venegas, F.C., Favia, M., Viola, A., Castegna, A., 2021. Reactive oxygen species in macrophages: sources and targets. Front. Immunol. 12, 734229.

Capparelli, M.V., Molinero, J., Moulatlet, G.M., Barrado, M., Prado-Alcívar, S., Cabrera, M., Gimiliani, G., Ñacato, C., Pinos-Velez, V., Cipriani-Avila, I., 2021. Microplastics in rivers and coastal waters of the province of Esmeraldas, Ecuador. Mar. Pollut. Bull. 173, 113067.

Cazón, P., Vázquez, M., 2019. Applications of chitosan as food packaging materials. In: Sustainable agriculture reviews 36: chitin and chitosan: applications in food, agriculture, pharmacy, medicine and wastewater treatment, pp. 81–123.

Cazón, P., Vázquez, M., 2020. Mechanical and barrier properties of chitosan combined with other components as food packaging film. Environ. Chem. Lett. 18 (2), 257–267.

Chen, G., Feng, Q., Wang, J., 2020. Mini-review of microplastics in the atmosphere and their risks to humans. Sci. Total Environ. 703, 135504.

Chen, H., Chen, X., Song, T.Y., Ge, J.Q., 2022. Expression profiles of zebrafish (Danio rerio) lysozymes and preparation of c-type lysozyme with high bacteriolytic activity against vibrio vulnificus. Antibiotics 11 (12), 1803.

Chien, P.J., Sheu, F., Huang, W.T., Su, M.S., 2007. Effect of molecular weight of chitosans on their antioxidative activities in apple juice. Food Chem. 102 (4), 1192–1198.

Colín-García, K., Elizalde-Velázquez, G.A., Gómez-Oliván, L.M., García-Medina, S., 2023. Influence of sucralose, acesulfame-k, and their mixture on brain's fish: a study of behavior, oxidative damage, and acetylcholinesterase activity in Danio rerio. Chemosphere 340, 139928.

Cui, J., Zhang, Y., Liu, L., Zhang, Q., Xu, S., Guo, M.Y., 2023. Polystyrene microplastics induced inflammation with activating the TLR2 signal by excessive accumulation of ROS in hepatopancreas of carp (Cyprinus carpio). Ecotoxicol. Environ. Saf. 251, 114539.

Dai, T., Tanaka, M., Huang, Y.Y., Hamblin, M.R., 2011. Chitosan preparations for wounds and burns: antimicrobial and wound-healing effects. Expert Rev. Anti Infect. Ther. 9 (7), 857–879.

Das, A., 2023. The emerging role of microplastics in systemic toxicity: involvement of reactive oxygen species (ROS). Sci. Total Environ. 165076.

Delgado-Aguilar, M., Puig, R., Sazdovski, I., Fullana-i-Palmer, P., 2020. Polylactic acid/polycaprolactone blends: on the path to circular economy, substituting single-use commodity plastic products. Materials 13 (11), 2655.

Dikgang, J., Leiman, A., Visser, M., 2012. Analysis of the plastic-bag levy in South Africa. Resources, Conservation and Recycling 66, 59–65.

Elizalde-Velázquez, G.A., Gómez-Oliván, L.M., 2021. Microplastics in aquatic environments: a review on occurrence, distribution, toxic effects, and implications for human health. Sci. Total Environ. 780, 146551.

Elizalde-Velázquez, G.A., Gómez-Oliván, L.M., García-Medina, S., Hernández-Díaz, M., Islas-Flores, H., Galar-Martínez, M., Hernández-Varela, J.D., 2022. Polystyrene microplastics mitigate the embryotoxic damage of metformin and guanylurea in Danio rerio. Sci. Total Environ. 852, 158503.

Emadian, S.M., Onay, T.T., Demirel, B., 2017. Biodegradation of bioplastics in natural environments. Waste Manag. 59, 526–536.
Fan, J., Zou, L., Duan, T., Qin, L., Qi, Z., Sun, J., 2022. Occurrence and distribution of microplastics in surface water and sediments in China's inland water systems: a critical review. J. Clean. Prod. 331, 129968.
Funkhouser, J.D., Aronson, N.N., 2007. Chitinase family GH18: evolutionary insights from the genomic history of a diverse protein family. BMC Evol. Biol. 7, 1–16.
Garcia, J.M., Robertson, M.L., 2017. The future of plastics recycling. Science 358 (6365), 870–872.
Gheorghita, R., Gutt, G., Amariei, S., 2020. The use of edible films based on sodium alginate in meat product packaging: an eco-friendly alternative to conventional plastic materials. Coatings 10 (2), 166.
Gutiérrez-Noya, V.M., Gómez-Oliván, L.M., Casas-Hinojosa, I., García-Medina, S., Rosales-Pérez, K.E., Orozco-Hernández, J.M., Islas-Flores, H., 2023. Short-term exposure to dexamethasone at environmentally relevant concentrations impairs embryonic development in Cyprinus carpio: bioconcentration and alteration of oxidative stress-related gene expression patterns. Sci. Total Environ. 898, 165528.
Hartmann, N.B., Hüffer, T., Thompson, R.C., Hassellöv, M., Verschoor, A., Daugaard, A. E., Rist, S., Karlsson, T., Brennholt, N., Cole, M., Herrling, M.P., Hess, M.C., Ivleva, N. P., Lusher, A.L., Wagner, M., 2019. Are we speaking the same language? Recommendations for a definition and categorization framework for plastic debris. Environ. Sci. Technol. 53 (3), 1039–1047. https://doi.org/10.1021/acs.est.8b05297. Feb 5. Epub 2019 Jan 17. PMID: 30608663.
Hasan, M., Gopakumar, D.A., Olaiya, N.G., Zarlaida, F., Alfian, A., Aprinasari, C., Khalil, H.A., 2020. Evaluation of the thermomechanical properties and biodegradation of brown rice starch-based chitosan biodegradable composite films. Int. J. Biol. Macromol. 156, 896–905.
Hernandez, O.C., Enrique, Á., Ward, R., Rodríguez-Santiago, M., Aguirre-Téllez, J.A., 2021. Microplastic distribution in urban vs pristine mangroves: using marine sponges as bioindicators of environmental pollution. Environ. Pollut. 284, 117391.
Hernández-Varela, J.D., Chanona-Pérez, J.J., Resendis-Hernández, P., Victoriano, L.G., Méndez-Méndez, J.V., Cárdenas-Pérez, S., Benavides, H.C., 2022. Development and characterization of biopolymers films mechanically reinforced with garlic skin waste for fabrication of compostable dishes. Food Hydrocoll. 124, 107252.
Herrera-Vázquez, S.E., Dublán-García, O., Arizmendi-Cotero, D., Gómez-Oliván, L.M., Islas-Flores, H., Hernández-Navarro, M.D., Ramírez-Durán, N., 2022. Optimization of the physical, optical and mechanical properties of composite edible films of gelatin, whey protein and chitosan. Molecules 27 (3), 869.
Hu, Q., Wang, H., He, C., Jin, Y., Fu, Z., 2021. Polystyrene nanoparticles trigger the activation of p38 MAPK and apoptosis via inducing oxidative stress in zebrafish and macrophage cells. Environ. Pollut. 269, 116075.
Huang, M., Khor, E., Lim, L.Y., 2004. Uptake and cytotoxicity of chitosan molecules and nanoparticles: effects of molecular weight and degree of deacetylation. Pharm. Res. 21, 344–353.
Issahaku, I., Tetteh, I.K., Tetteh, A.Y., 2023. Chitosan and chitosan derivatives: recent advancements in production and applications in environmental remediation. Environmental Advances 11, 100351.
Jeong, C.B., Kang, H.M., Lee, M.C., Kim, D.H., Han, J., Hwang, D.S., Lee, J.S., 2017. Adverse effects of microplastics and oxidative stress-induced MAPK/Nrf2 pathway-mediated defense mechanisms in the marine copepod Paracyclopina nana. Sci. Rep. 7 (1), 41323.
Jiang, Z.Y., Hunt, J.V., Wolff, S.P., 1992. Ferrous ion oxidation in the presence of xylenol orange for detection of lipid hydroperoxide in low density lipoprotein. Anal. Biochem. 202, 384–389.
Jin, Y., Xia, J., Pan, Z., Yang, J., Wang, W., Fu, Z., 2018. Polystyrene microplastics induce microbiota dysbiosis and inflammation in the gut of adult zebrafish. Environ. Pollut. 235, 322–329.
Ju, S., Shin, G., Lee, M., Koo, J.M., Jeon, H., Ok, Y.S., Park, J., 2021a. Biodegradable chito-beads replacing non-biodegradable microplastics for cosmetics. Green Chem. 23 (18), 6953–6965.
Ju, S., Shin, G., Lee, M., Koo, J.M., Jeon, H., Ok, Y.S., Park, J., 2021b. Biodegradable chito-beads replacing non-biodegradable microplastics for cosmetics. Green Chem. 23 (18), 6953–6965.
Kean, T., Thanou, M., 2010a. Biodegradation, biodistribution and toxicity of chitosan. Adv. Drug Deliv. Rev. 62 (1), 3–11.
Kean, T., Thanou, M., 2010b. Biodegradation, biodistribution and toxicity of chitosan. Adv. Drug Deliv. Rev. 62 (1), 3–11.
Kean, T., Thanou, M., 2011. Chitin and Chitosan: Sources, Production and Medical Applications.
Kim, D.S., Yang, X., Lee, J.H., Yoo, H.Y., Park, C., Kim, S.W., Lee, J., 2022. Development of GO/co/chitosan-based nano-biosensor for real-time detection of D-glucose. Biosensors 12 (7), 464.
Kye, H., Kim, J., Ju, S., Lee, J., Lim, C., Yoon, Y., 2023. Microplastics in water systems: a review of their impacts on the environment and their potential hazards. Heliyon 9 (3), e14359. https://doi.org/10.1016/j.heliyon.2023.e14359. Mar 7. PMID: 36950574; PMCID: PMC10025042.
Lee, J.H., Kang, J.C., Kim, J.H., 2023. Toxic effects of microplastic (polyethylene) on fish: accumulation, hematological parameters and antioxidant responses in Korean bullhead, Pseudobagrus fulvidraco. Sci. Total Environ. 877, 162874.
Levine, R.L., Williams, J.A., Stadtman, E.R., Shacter, E., 1994. Carbonyl assays for determination of oxidatively modified proteins. Methods Enzymol. 233, 346–357.
Li, S., Li, C., Wu, S., 2022. Dietary chitosan modulates the growth performance, body composition and nonspecific immunity of juvenile yellow catfish (Pelteobagrus fulvidraco). Int. J. Biol. Macromol. 217, 188–192.
Makarios-Laham, I., Lee, T.C., 1995. Biodegradability of chitin-and chitosan-containing films in soil environment. Journal of environmental polymer degradation 3, 31–36.
Malafeev, K.V., Apicella, A., Incarnato, L., Scarfato, P., 2023. Understanding the impact of biodegradable microplastics on living organisms entering the food chain: a review. Polymers 15 (18), 3680.
Martins, S.H.F., Pontes, K.V., Fialho, R.L., Fakhouri, F.M., 2022. Extraction and characterization of the starch present in the avocado seed (Persea americana mill) for future applications. Journal of Agriculture and Food Research 8, 100303.
Meng, X., Yin, K., Zhang, Y., Wang, D., Lu, H., Hou, L., Xing, M., 2022. Polystyrene microplastics induced oxidative stress, inflammation and necroptosis via NF-κB and RIP1/RIP3/MLKL pathway in chicken kidney. Toxicology 478, 153296.
Misra, H.P., Fridovich, I., 1972. The role of superoxide anion in the autoxidation of epinephrine and a simple assay for superoxide dismutase. J. *Biol. Chem.* 247, 3170–3175.
Mitrano, D.M., Wohlleben, W., 2020. Microplastic regulation should be more precise to incentivize both innovation and environmental safety. Nat. Commun. 11 (1), 5324.
Namphonsane, A., Suwannachat, P., Chia, C.H., Wongsagonsup, R., Smith, S.M., Amornsakchai, T., 2023. Toward a circular bioeconomy: exploring pineapple stem starch film as a plastic substitute in single use applications. Membranes 13 (5), 458.
Ogunola, O.S., Onada, O.A., Falaye, A.E., 2018. Mitigation measures to avert the impacts of plastics and microplastics in the marine environment (a review). Environ. Sci. Pollut. Res. 25, 9293–9310.
Opanasopit, P., Aumklad, P., Kowapradit, J., Ngawhiranpat, T., Apirakaramwong, A., Rojanarata, T., Puttipipatkhachorn, S., 2007. Effect of salt forms and molecular weight of chitosans on in vitro permeability enhancement in intestinal epithelial cells (Caco-2). Pharm. Dev. Technol. 12 (5), 447–455.
Pan, Y., Gao, S.H., Ge, C., Gao, Q., Huang, S., Kang, Y., Wang, A.J., 2023. Removing microplastics from aquatic environments: a critical review. Environmental Science and Ecotechnology 13, 100222.
Park, P.J., Je, J.Y., Kim, S.K., 2004. Free radical scavenging activities of differently deacetylated chitosans using an ESR spectrometer. Carbohydr. Polym. 55 (1), 17–22.
Park, P.J., Koppula, S., Kim, S.K., 2010. 18 Antioxidative Activity of Chitosan, Chitooligosaccharides and Their Derivatives. Chitin, chitosan, oligosaccharides and their derivatives, 241.
Pfaffl, M.W., 2001. A new mathematical model for relative quantification in real-time RT–PCR. Nucleic Acids Res. 29 (9), e45.
Pfaffl, M.W., Horgan, G.W., Dempfle, L., 2002. Relative expression software tool (REST©) for group-wise comparison and statistical analysis of relative expression results in real-time PCR. Nucleic Acids Res. 30 (9), e36.
Pettipas, S., Bernier, M., Walker, T.R., 2016. A Canadian policy framework to mitigate plastic marine pollution. Mar. Policy 68, 117–122.
Radi, R., Turrens, J.F., Chang, L.Y., Bush, K.M., Carpo, J.D., Freeman, B.A., 1991. Detection of catalase in rat heart mitochondria. J. *Biol. Chem.* 266, 22028–22034.
Sanchez, W., Burgeot, T., Porcher, J.M., 2013. A novel "integrated biomarker response" calculation based on reference deviation concept. Environ. Sci. Pollut. Res. 20, 2721–2725.
Schmittgen, T.D., Livak, K.J., 2008. Analyzing real-time PCR data by the comparative CT method. Nat. Protoc. 3 (6), 1101–1108.
Sewwandi, M., Wijesekara, H., Rajapaksha, A.U., Soysa, S., Vithanage, M., 2023. Microplastics and plastics-associated contaminants in food and beverages; global trends, concentrations, and human exposure. Environ. Pollut. 317, 120747.
Shang, Y., Wang, X., Chang, X., Sokolova, I.M., Wei, S., Liu, W., Wang, Y., 2021. The effect of microplastics on the bioenergetics of the mussel Mytilus coruscus assessed by cellular energy allocation approach. Front. Mar. Sci. 8, 754789.
Shejkar, S.K., Agrawal, A., Agrawal, B., 2020. Walnut shell particulates as filler material in polymeric matrix: a review. Int. J. Eng. Res. Curr. Trends (IJERCT) 2 (3), 41–43.
Teng, Z., Sun, C., Liu, S., Wang, H., Zhang, S., 2014. Functional characterization of chitinase-3 reveals involvement of chitinases in early embryo immunity in zebrafish. Developmental & Comparative Immunology 46 (2), 489–498.
Unuofin, J.O., Igwaran, A., 2023. Microplastics in seafood: implications for food security, safety, and human health. J. Sea Res. 194, 102410.
Usman, S., Abdull Razis, A.F., Shaari, K., Amal, M.N.A., Saad, M.Z., Mat Isa, N., Nazarudin, M.F., 2021. Polystyrene microplastics exposure: an insight into multiple organ histological alterations, oxidative stress and neurotoxicity in Javanese medaka fish (Oryzias javanicus Bleeker, 1854). Int. J. Environ. Res. Public Health 18 (18), 9449.
Van Roijen, E.C., Miller, S.A., 2022. A review of bioplastics at end-of-life: linking experimental biodegradation studies and life cycle impact assessments. Resour. Conserv. Recycl. 181, 106236.
Verma, D., Okhawilai, M., Goh, K.L., Thakur, V.K., Senthilkumar, N., Sharma, M., Uyama, H., 2023. Sustainable functionalized chitosan based nano-composites for wound dressings applications: a review. Environ. Res. 116580.
Vitali, C., Peters, R.J., Janssen, H.G., Nielen, M.W., 2023. Microplastics and nanoplastics in food, water, and beverages; part I. Occurrence. TrAC Trends in Analytical Chemistry 159, 116670.
Wang, J., Li, Y., Lu, L., Zheng, M., Zhang, X., Tian, H., Ru, S., 2019. Polystyrene microplastics cause tissue damages, sex-specific reproductive disruption and transgenerational effects in marine medaka (Oryzias melastigma). Environ. Pollut. 254, 113024.
Wei, S., Ching, Y.C., Chuah, C.H., 2020. Synthesis of chitosan aerogels as promising carriers for drug delivery: a review. Carbohydr. Polym. 231, 115744.
Yan, J., Guo, C., Dawood, M.A.O., Gao, J., 2017. Effects of dietary chitosan on growth, lipid metabolism, immune response and antioxidant-related gene expression in Misgurnus anguillicaudatus. Benefic. Microbes 8 (3), 439–449.
Yang, S., Lian, G., 2020. ROS and diseases: role in metabolism and energy supply. Mol. Cell. Biochem. 467, 1–12.

Yang, Y.M., Hu, W., Wang, X.D., Gu, X.S., 2007. The controlling biodegradation of chitosan fibers by N-acetylation in vitro and in vivo. J. Mater. Sci. Mater. Med. 18, 2117–2121.
Yang, L., Zhang, Y., Kang, S., Wang, Z., Wu, C., 2021. Microplastics in soil: a review on methods, occurrence, sources, and potential risk. Sci. Total Environ. 780, 146546.
Yin, L., Chen, B., Xia, B., Shi, X., Qu, K., 2018. Polystyrene microplastics alter the behavior, energy reserve and nutritional composition of marine jacopever (Sebastes schlegelii). J. Hazard. Mater. 360, 97–105.
Yuan, W., Liu, X., Wang, W., Di, M., Wang, J., 2019. Microplastic abundance, distribution and composition in water, sediments, and wild fish from Poyang Lake, China. Ecotoxicol. Environ. Saf. 170, 180–187.
Zhao, J., Qiu, P., Wang, Y., Wang, Y., Zhou, J., Zhang, B., Gou, D., 2023. Chitosan-based hydrogel wound dressing: from mechanism to applications, a review. Int. J. Biol. Macromol. 125250.
Zuri, G., Karanasiou, A., Lacorte, S., 2023. Microplastics: human exposure assessment through air, water, and food. Environ. Int. 179, 108150.